nature neuroscience

Activity-dependent PSA expression regulates inhibitory maturation and onset of critical period plasticity

Graziella Di Cristo[1,6], Bidisha Chattopadhyaya[1,2,6], Sandra J Kuhlman[1], Yu Fu[1], Marie-Claude Bélanger[3], Cai Zhi Wu[1], Urs Rutishauser[4], Lamberto Maffei[5] & Z Josh Huang[1]

Functional maturation of GABAergic innervation in the developing visual cortex is regulated by neural activity and sensory inputs and in turn influences the critical period of ocular dominance plasticity. Here we show that polysialic acid (PSA), presented by the neural cell adhesion molecule, has a role in the maturation of GABAergic innervation and ocular dominance plasticity. Concentrations of PSA significantly decline shortly after eye opening in the adolescent mouse visual cortex; this decline is hindered by visual deprivation. The developmental and activity-dependent regulation of PSA expression is inversely correlated with the maturation of GABAergic innervation. Premature removal of PSA in visual cortex results in precocious maturation of perisomatic innervation by basket interneurons, enhanced inhibitory synaptic transmission, and earlier onset of ocular dominance plasticity. The developmental and activity-dependent decline of PSA expression therefore regulates the timing of the maturation of GABAergic inhibition and the onset of ocular dominance plasticity.

The PSA moiety is a long, linear homopolymer of α-2,8-linked sialic acid attached almost exclusively to the neural cell adhesion molecule (NCAM) in vertebrates[1]. Owing to its polyanionic structure and large hydrated volume[2], PSA in abundance at the cell surface modulates cell-cell bonds mediated not only by NCAM but also by various other adhesion molecules[3,4]. The modulation of PSA expression influences a wide range of structural changes in cell position and shape in the nervous system. Indeed, PSA has been implicated in neuronal migration[5,6], axonal fasciculation, branching, guidance[7–13], synaptogenesis[8,14] and activity-dependent plasticity[15–17]. A common theme is that PSA does not by itself provide a specific instructive cue but rather acts as a regulated permissive signal in morphogenesis. The coupling of changes in PSA expression with the relevant neural developmental process seems to be a crucial factor in creating permissive conditions for the growth and refinement of neuronal connections at the appropriate time and place[18]. PSA is widely expressed in postnatal rodent neocortex, but its function in local cortical circuit formation and plasticity is unclear. In particular, it is unknown whether PSA plays a part in the development of GABAergic inhibitory synapses in visual cortex.

GABAergic inhibition regulates neuronal excitability[19], synaptic integration[20], neuronal network activity[21,22] and neural plasticity[23–25]. GABAergic interneuron axons in neocortex are characterized by their local exuberance in innervating specific cellular and subcellular targets[26]; this innervation allows the distribution of inhibitory outputs to discrete spatial domains in local circuits. The maturation of GABAergic innervation and functional inhibition in visual cortex is a protracted process, extending well into adolescence, and is regulated by neural activity and visual experience[27,28]. Maturation of inhibition, in turn, influences the onset and time course of ocular dominance plasticity[24,25], representing a classic example of experience-dependent refinement of neuronal connections. During a postnatal critical period, closure of one eye causes the binocular neurons in primary visual cortex to shift their responsiveness toward input from the open eye[23]. By regulating the onset of the critical period, GABAergic interneurons may influence how experience shapes neuronal circuits in the visual cortex during early postnatal life.

Several studies have begun to elucidate the molecular mechanisms that mediate activity-dependent maturation of GABAergic innervation. For instance, the neurotrophin BDNF has been shown to promote the maturation of GABAergic innervation, including GABAergic synapses targeted to the perisomatic region of pyramidal neurons[29]. In addition, studies have implicated GABA synthesis and signaling mediated by the glutamic acid decarboxylase GAD67 in the activity-dependent maturation of perisomatic GABAergic innervation[30]. Although some of the factors that stimulate the maturation of GABAergic innervation have been identified, it is unknown whether there are also inhibitory mechanisms that contribute to the establishment of GABAergic innervation patterns and to the appropriate time course of their maturation. For example, it is not clear whether the reduction in GABAergic inhibition that follows visual deprivation results from a downregulation of stimulatory factors or a retention of inhibitory factors.

[1]Cold Spring Harbor Laboratory, 1 Bungtown Road, Cold Spring Harbor, New York 11734, USA. [2]Neuroscience Program, State University of New York, Stony Brook, New York 11790, USA. [3]Centre Hospitalier Universitaire (CHU) Sainte-Justine – Université de Montréal, 3715 Côte-Ste-Catherine, Montreal H3T IC5, Canada. [4]Memorial Sloan-Kettering Cancer Center, 1275 York Avenue, New York 10021, USA. [5]Instituto di Neurofisiologia del Centro Nazionale della Ricerca, via G. Moruzzi 1, 56124 Pisa, Italy. [6]Present addresses: CHU Sainte-Justine – Université de Montréal, Montreal, Quebec, Canada (G.D.C.); Friedrich Miescher Institute, Novartis Research Foundation, Basel, Switzerland (B.C.). Correspondence should be addressed to Z.J.H. (huangj@cshl.edu).

Received 26 July; accepted 5 October; published online 18 November 2007; doi:10.1038/nn2008

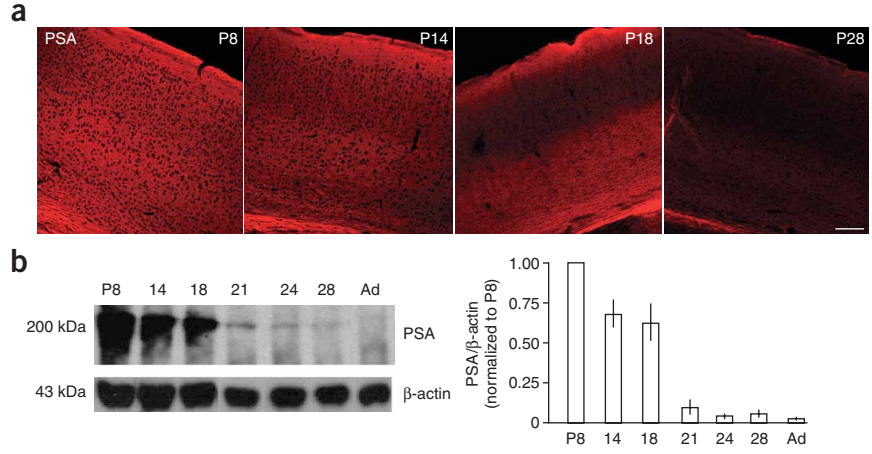

Figure 1 PSA expression declines shortly after eye opening in mouse visual cortex. (**a**) Coronal sections from visual cortex at different ages immunostained with antibodies to PSA (anti-PSA). PSA is highly expressed at P8 but is almost undetectable after the fourth postnatal week. (**b**) Left, immunoblot analysis of visual cortex using anti-PSA (top) and anti–β-actin (bottom) shows that PSA declines rapidly shortly after eye opening (P14). The PSA band is broad because NCAM, the PSA carrier protein, has several isoforms characterized by different molecular mass. Molecular masses are indicated in kilodaltons on the left. Right, quantification of immunoblot. For each sample, the PSA signal was first normalized to the β-actin signal. Bar graph shows mean ± s.d. for each time point normalized to P8 ($n = 3$ mice for each time point). Ad, adult, 8–10 weeks. Scale bar, 200 μm.

Here we have examined the role of PSA in the activity-dependent maturation of GABAergic inhibition in adolescent visual cortex, focusing on the perisomatic synapses formed by basket interneurons. We show that PSA expression is downregulated in visual cortex after eye opening and its decline is dependent on sensory experience. Premature removal of PSA induces precocious maturation of perisomatic GABAergic innervation and onset of the critical period for ocular dominance plasticity. Our data indicate that visual activity–dependent PSA expression may regulate the timing of the maturation of perisomatic GABAergic innervation and the onset of ocular dominance plasticity, thereby defining a role for PSA in local circuit development in the adolescent neocortex.

RESULTS

Developmental and experience-dependent PSA expression

We first characterized the time course of PSA and NCAM expression during postnatal development in mouse visual cortex by using immunofluorescence and immunoblot analysis. Both PSA and NCAM were highly expressed in all layers of the neonatal visual cortex. In particular, our data showed that PSA is broadly expressed in all cortical layers (**Fig. 1** and **Supplementary Fig. 1** online), with higher expression in layers 4 and 5/6, consistent with a previous report[11]. Expression of PSA then steadily decreased in subsequent postnatal weeks, with a sharp decline in all cortical layers shortly after eye opening at about postnatal day 14 (P14; **Fig. 1**; one-way analysis of variance (ANOVA), $P < 0.05$). This decline continued into the fourth postnatal week. In fact, even

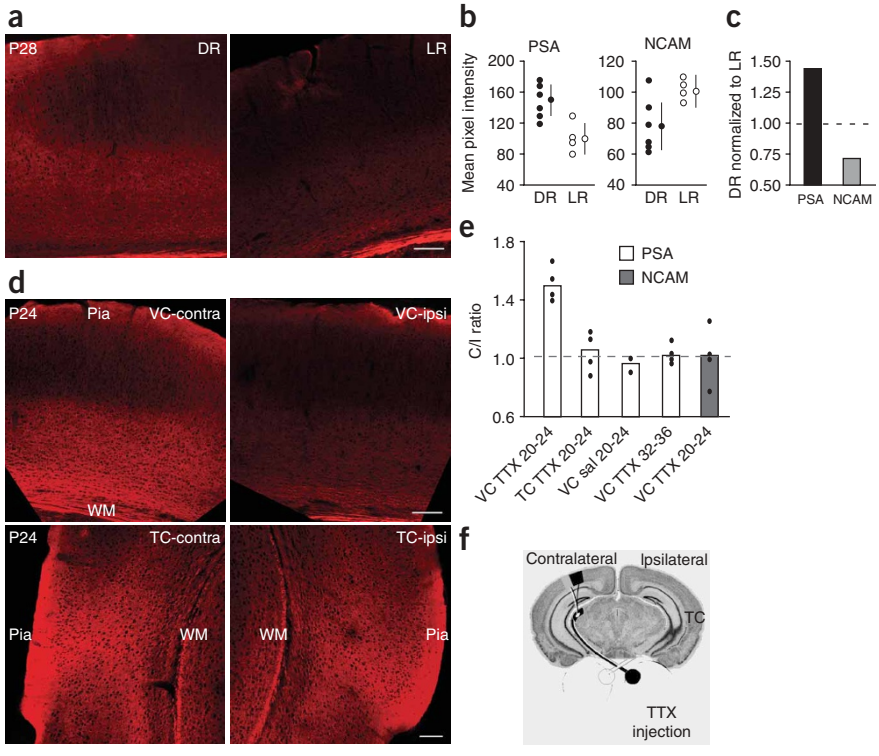

Figure 2 Visual experience downregulates PSA expression in mouse visual cortex. (**a**–**c**) Dark rearing (from birth to P28) prevents the developmental downregulation of PSA but not NCAM. (**a**) PSA is higher in the visual cortex (VC) of DR mice than in that of LR littermates. (**b**) Quantification of PSA and NCAM as mean pixel intensity, plotted for each mouse along with mean ± s.d. for each experimental condition. PSA in the VC is significantly higher (*t*-test, $P < 0.01$), whereas NCAM is lower, in DR mice than in LR littermates (*t*-test, $P < 0.05$). (**c**) Expression of PSA and NCAM in the VC of DR mice normalized to that of LR littermates. Bar indicates average values. (**d**–**f**) Daily monocular TTX injection from P20 to P24, but not from P32 to P36, prevents developmental downregulation of PSA in binocular primary VC. (**d**) In the VC ipsilateral to TTX injection (nondeprived, VC-ipsi), PSA is consistently lower than in the contralateral, deprived VC (VC-contra), but PSA is unaffected in the nearby temporal cortex (TC-contra and TC-ipsi). (**e**) Effects of monocular TTX injection on PSA (white) and NCAM (gray) expression in the contralateral (deprived) cortex normalized to ipsilateral (nondeprived) cortex. Filled circles represent values from each mouse; histogram indicates average values. TTX injection between P20 and P24 (TTX 20–24) increases PSA, but not NCAM, in the deprived visual cortex, but does not affect PSA in the nearby temporal cortex. Neither saline (sal 20–24) nor TTX injection between P32 and P36 affects PSA (deprived versus nondeprived cortex, *t*-test, $P < 0.01$ only for PSA in VC TTX 20–24). (**f**) Monocular TTX injection. Scale bar, 200 μm. WM, white matter.

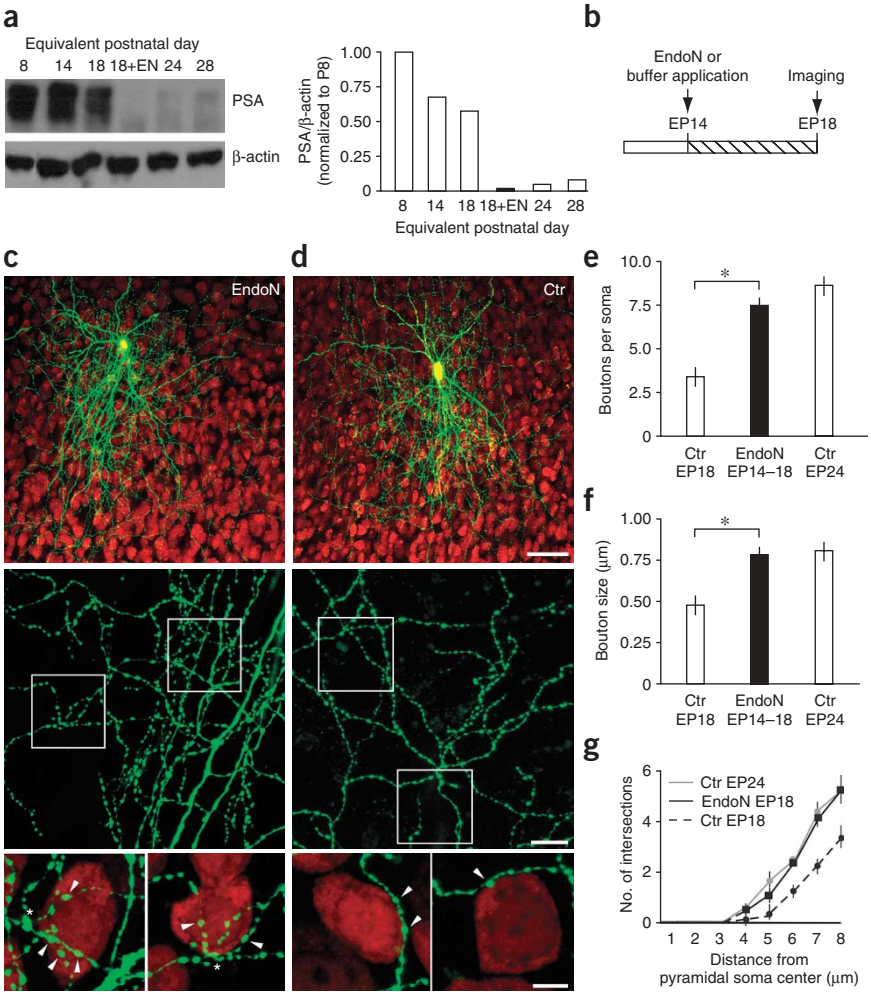

Figure 3 Premature reduction of PSA expression promotes maturation of perisomatic GABAergic synapses in cortical organotypic cultures. (**a**) Left, PSA in cortical organotypic cultures decreases markedly after 2 weeks *in vitro* with a time course similar to that in visual cortex (compare **Fig. 1b**). EndoN application in the culture medium from EP14 to EP18 depletes PSA expression (18+EN). Right, quantification of immunoblot as in **Figure 1b** ($n = 4$–6 cortical organotypic slices for each time point). (**b**) Experimental protocol. (**c**,**d**) As compared with an age-matched control basket cell (**d**), an EndoN-treated basket cell (**c**) shows significantly increased axon branching (middle), terminal branching around pyramidal somata (**c**, bottom, asterisk) and perisomatic bouton density (bottom, arrowheads). Pyramidal somata are labeled with an antibody to NeuN (red). Bottom panels are magnifications of boxed regions in middle panels. Scale bars, 50 μm (top); 10 μm (middle); 5 μm (bottom). (**e**–**f**) Perisomatic bouton density and size from EndoN-treated basket cells (8 basket cells and 55 pyramidal somata) are increased as compared with aged-matched controls (7 basket cells and 42 pyramidal somata; one-way ANOVA, *post hoc* Dunn's test, $P < 0.05$) and comparable to those from a more mature stage (EP24, 7 basket cells and 52 pyramidal somata; one-way ANOVA, *post hoc* Dunn's test, $P > 0.05$). Graphs represent mean ± s.e.m. * indicate $P < 0.05$. (**g**) EndoN-treated basket cells show increased terminal branching complexity as compared with control cells, as quantified by reverse three-dimensional Sholl analysis[27] (one-way ANOVA, *post hoc* Dunn's test, $P < 0.05$).

though the difference in PSA between P21 and P28 did not reach significance in the immunoblot analysis (one-way ANOVA, Dunn's *post hoc* test, $P > 0.05$), PSA immunofluorescence was still clearly visible in layer 56 of the visual cortex at P24 (**Fig. 2**, VC-ipsi), including around GABAergic axon terminals (**Supplementary Fig. 2** online). Whereas NCAM expression was maintained in substantial amounts in P32 and adult mice (**Supplementary Fig. 1** and data not shown), PSA was barely detectable after the fourth postnatal week (**Fig. 1b**). The sharp decline in PSA shortly after eye opening suggests that visual experience has a role in the developmental downregulation of PSA.

To examine this possibility, we reared mouse pups in the dark from birth and quantified PSA and NCAM in the visual cortex at P28. As compared with littermates reared under a normal light/dark cycle (LR mice), dark-reared pups (DR mice) showed significantly higher PSA expression (**Fig. 2a–c**; 44% higher mean pixel intensity versus LR mice; LR mice, $n = 4$; DR mice, $n = 6$; *t*-test, $P < 0.01$). By contrast, we observed a reduction in NCAM in the visual cortex of DR mice (**Fig. 2b**,**c**; 30% reduction in mean pixel intensity; *t*-test, $P < 0.05$). Even though PSA expression is consistently higher in layers 4 and 5/6 as reported by others[11], a similar extent of reduction was observed in supragranular (data not shown) and infragranular (**Fig. 2b**) layers in DR as compared with LR mice. This result suggests that visual experience may regulate PSA expression. In addition to visual deprivation[31], however, prolonged dark rearing could result in other physiological and behavioral effects that might affect PSA and NCAM expression.

To further examine the role of visual experience, we injected 3 mM tetrodotoxin (TTX) daily into one eye of mice from P20 to P24, a stage when PSA is declining in visual cortex (**Fig. 2d–f**), and then quantified PSA and NCAM expression in the binocular regions of primary visual cortex in the two hemispheres, blind to the site of TTX injection. Expression of PSA, but not NCAM, was higher in the binocular region contralateral to the injected eye (deprived cortex) than in the ispilateral region (nondeprived cortex; **Fig. 2d**,**e**; mean ± s.e.m. contralateral/ipsilateral (C/I) ratio: PSA, 152 ± 6%, *t*-test, $P < 0.01$; NCAM, 101 ± 20%; *t*-test, $P > 0.1$; $n = 4$ mice). The relative increase in PSA was similar in the supra- and infragranular layers. These effects were specific to the visual cortex, because PSA expression in the contralateral temporal cortex was not different from that in the temporal cortex ipsilateral to the deprived eye (**Fig. 2d**,**e**; C/I ratio = 104 ± 8%, *t*-test, $P > 0.1$). Buffer injection alone did not affect PSA expression (**Fig. 2e**; C/I ratio = 95 ± 4%, $n = 2$, *t*-test, $P > 0.1$). The efficacy of visual deprivation to prevent the developmental downregulation of PSA was restricted to a critical time window because TTX injection from P32 to P36 was not effective (**Fig. 2e**; C/I ratio for PSA = 99 ± 4%; $n = 4$ mice; *t*-test $P > 0.1$). Together, these results indicate that the downregulation of PSA, but not NCAM itself, during postnatal development is influenced by visual experience.

PSA removal promotes maturation in culture GABAergic synapse

The developmental and experience-dependent regulation of PSA expression is inversely correlated with the maturation of GABAergic innervation during the same period in visual cortex[27,28], suggesting that

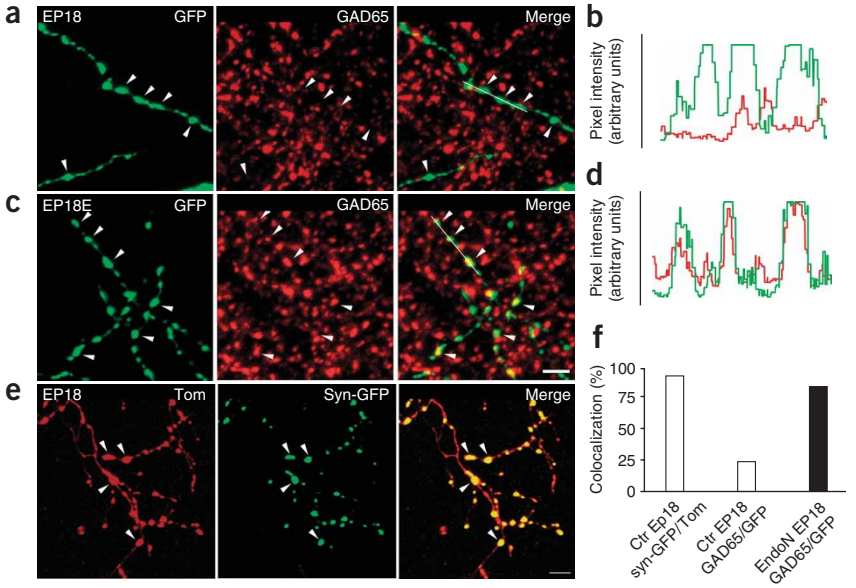

Figure 4 Premature reduction of PSA expression promotes localization of GAD65 to presynaptic boutons of basket cells. (**a**–**d**) Localization of GAD65 (red) in the presynaptic boutons (arrowheads) is increased in EndoN-treated basket cells (**c**) as compared with age-matched controls (**a**) at EP18. Plots of pixel intensity for GFP (green) and GAD65 (red) immunofluorescence along the indicated white line show significantly higher GAD65 signals in EndoN-treated basket cell boutons (**d**) than in control basket cells boutons (**b**). (**e**) A basket cell is co-transfected with P_{G67}-tdtomato (Tom; left, red) and P_{G67}-syn-GFP (middle, green) to simultaneously visualize axon-bouton morphology and a synaptic marker at EP18. Most tdtomato-labeled boutons contain syn-GFP (right, arrowheads). Scale bar, 5 μm. (**f**) Quantification shows that 95.3% of basket cell boutons contain syn-GFP at EP18 (273 boutons from 3 cells), whereas only 22% colocalize with GAD65 immunostaining (110 boutons, 3 cells). EndoN treatment from EP14 to EP18 increases the proportion of GAD65-positive basket cell boutons to 81% (138 boutons from 3 cells).

higher PSA concentrations may hinder the maturation of GABAergic innervation. Indeed, PSA has been shown to inhibit axon branching[11] and may shield axons from inappropriate and premature interactions with its local environment[12,13]. To test this hypothesis, we first examined whether and how enzymatic removal of PSA with the highly specific endoneuraminidase EndoN[32] affects GABAergic innervation in cortical organotypic cultures. The basic features of perisomatic innervation of pyramidal cells by basket interneurons develop in organotypic culture[27,33,34]. In particular, perisomatic innervation matures significantly after the second postnatal week in culture and is influenced by alterations in neuronal activity[27]. PSA, quantified by immunoblot analysis, decreased over the same period in cortical organotypic cultures (**Fig. 3a**), with a sharp decline occurring after equivalent postnatal day 18 (EP18 = P4 + 14 d *in vitro*). This decline occurs in parallel to an increase in spontaneous activity[35].

To label single basket interneuron axons and synapses at high resolution, we used a previously characterized promoter region (P_{G67}) to express enhanced green fluorescent protein (EGFP) in

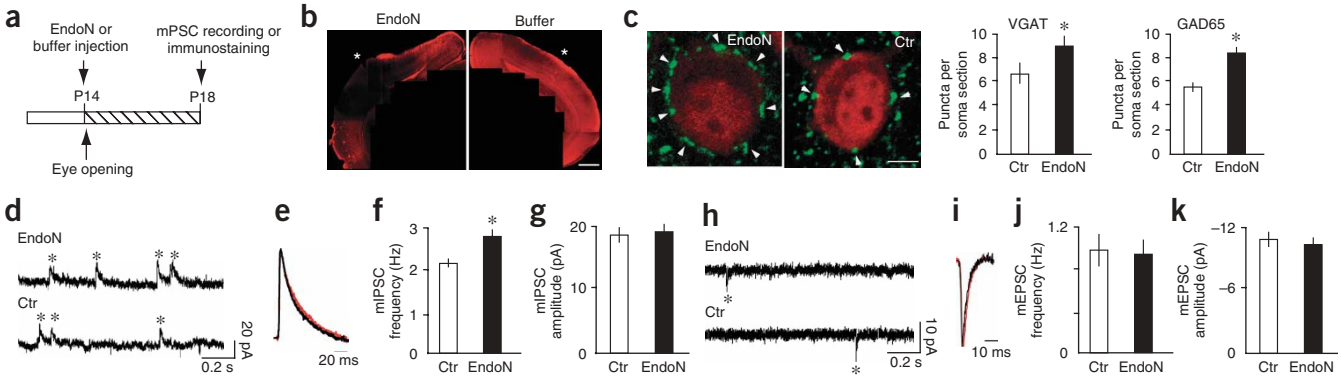

Figure 5 Premature reduction of PSA expression in visual cortex promotes functional maturation of GABAergic but not glutamatergic synapses. (**a**) Experimental protocol. (**b**) Coronal brain section from an EndoN-injected mouse shows a marked decrease in PSA (red) in visual cortex (left). Buffer injection does not affect PSA expression (right). Images are a composite of several high-magnification micrographs. Asterisk indicates injection site. (**c**) Mice injected with EndoN or vehicle immunostained with VGAT (left, green) or GAD65 (**Supplementary Fig. 3**) to visualize perisomatic boutons around pyramidal cell somata (NeuN, red). VGAT puncta (arrowheads) always form distinct ring-like structures around neuronal somata in EndoN-injected visual cortex (EndoN) but rarely do so in vehicle-injected controls (Ctr). Scale bar, 5 μm. The density of perisomatic VGAT and GAD65 puncta is higher in EndoN-injected cortex than in contralateral uninjected cortex ($n = 3$ mice; t-test, $P < 0.001$); there was no difference between the two cortices in vehicle-injected littermates (data not shown; $n = 3$ mice; t-test, $P > 0.1$). (**d**–**g**) Functional maturation of GABAergic synapses assessed by mIPSC recording from layer 5 pyramidal cells in visual cortex. (**d**) Examples of current traces recorded in an EndoN-treated and a control cell. (**e**) Superimposed normalized average traces of the mIPSCs recorded in all EndoN-treated (black) and control (red) cells. (**f**,**g**) EndoN application increases the frequency (**f**; t-test, $P < 0.01$), but not amplitude (**g**; t-test, $P > 0.1$), of mIPSC events as compared with age-matched controls ($n = 18$ cells from four mice for both groups), consistent with an increase in GABAergic synapse number. (**h**–**k**) Functional maturation of glutamatergic synapses assessed by mEPSC recording from layer 5 pyramidal cells in visual cortex. (**h**) Examples of current traces recorded in an EndoN-treated and a control cell. (**i**) Superimposed normalized average traces of the mEPSCs recorded in all EndoN-treated (black) and control (red) cells. (**j**,**k**) EndoN application affects neither the frequency (**j**; t-test, $P > 0.1$) nor the amplitude (**k**; t-test, $P > 0.1$) of mEPSC events (EndoN-treated, $n = 21$ cells from four mice; control, $n = 20$ cells from four mice). All graphs represent mean ± s.e.m. * indicate $P < 0.05$ in **c** and **f**, and single mPSC events in **d** and **h**.

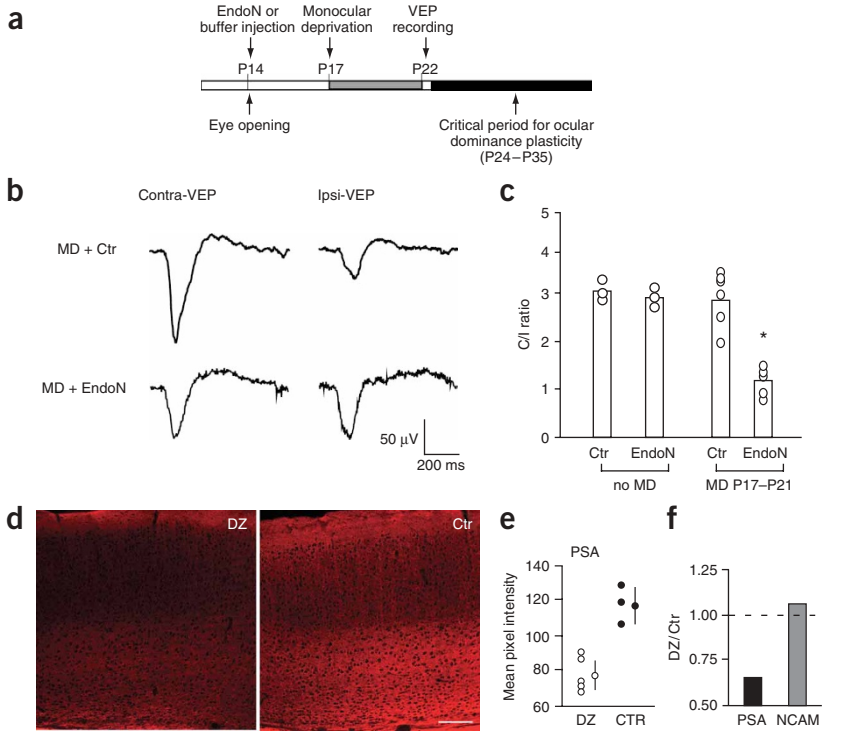

Figure 6 Premature reduction of PSA expression in visual cortex induces precocious onset of the critical period for ocular dominance plasticity. (**a**) Experimental protocol. (**b**) The contralateral eye is sutured from P17 to P22, before the normal onset of ocular dominance plasticity, as assessed by VEP. Shown are examples of VEPs from an EndoN- and a buffer-injected mouse, recorded from the binocular visual cortex, ~400 μm below the cortical surface. In controls, the VEP amplitudes induced by the contralateral eye input are larger than those induced by the ipsilateral eye input, indicating the characteristic contralateral bias and absence of ocular dominance shift. In EndoN-treated mice, the VEP amplitudes induced by the contralateral eye input are similar to those induced by the ipsilateral eye input, indicating a significant shift in ocular dominance. (**c**) Five days of monocular deprivation does not affect the C/I ratio in vehicle-injected mice (*t*-test, $P > 0.1$), but it induces a shift in ocular dominance in EndoN-injected mice (*t*-test, $P < 0.001$), indicating an early onset of the critical period for ocular dominance plasticity. Open circles represent values from each mouse; histogram indicates average values. (**d**–**f**) Daily intraventricular diazepam (DZ) injection from P15 to P19 decreases PSA. (**d**) PSA is lower in the visual cortex of DZ-injected mice as compared with vehicle-injected mice (Ctr). Scale bar, 100 μm. (**e**). Quantification of PSA. Mean pixel intensity is plotted for each mouse along with mean ± s.d. for each experimental condition. PSA in visual cortex is significantly lower in DZ-injected mice (*t*-test, $P < 0.01$). (**f**) PSA but not NCAM expression is reduced by DZ injections. Histogram represents mean PSA and NCAM expression in the visual cortex of DZ-injected mice normalized to that of control littermates.

parvalbumin-positive basket interneurons by means of biolistic transfection[27]. Fluorescence imaging and electron microscopy studies have shown that the GFP-positive boutons labeled by this method are presynaptic components of symmetric synapses[27,30]. Enzymatic removal of PSA with EndoN from EP14 to EP18 (**Fig. 3b**) resulted in premature elimination of PSA expression (**Fig. 3a**, '18 +E') and precocious maturation of perisomatic GABAergic synapses (**Fig. 3c–g**). In control EP18 cultures, the axon arbors of basket cells had reached almost mature size and overall geometry (**Fig. 3d**), but had not yet extended exuberant local branches, in particular the terminal branches around pyramidal cell somata (**Fig. 3d** middle and bottom). Basket axons also bore relatively sparse and small boutons (**Fig. 3d**, bottom). In EndoN-treated cultures, basket axons showed more extensive local branching; the most prominent feature was the appearance of highly distinct terminal forks around pyramidal cell somata with two or three terminal branches covered with larger and numerous regularly spaced boutons (**Fig. 3c,e,f,g**; mean ± s.e.m. boutons per soma: EndoN-treated cultures, 7.4 ± 0.5, $n = 55$ pyramidal somata from eight basket cells; control cultures, 3.4 ± 0.4, $n = 42$ pyramidal somata from seven basket cells; one-way ANOVA, *post hoc* Dunn's test, $P < 0.05$). EndoN-treated basket cells formed perisomatic synapses that were indistinguishable from those observed at more mature stages (**Fig. 3e,f,g**; EP24: boutons per soma, 8.5 ± 0.6, $n = 52$ pyramidal cell somata from seven basket cells; one-way ANOVA, *post hoc* Dunn's test, $P > 0.05$).

The GABA-synthesizing enzyme GAD65 is highly concentrated in mature presynaptic boutons[29,36], where it is involved in the rapid synthesis and release of GABA[37]. Overall, there is a developmental increase in GAD65 localization to presynaptic boutons from P14 to P28 in mouse visual cortex[29]. In mature organotypic cultures, GAD65 is similarly enriched in the presynaptic boutons of basket interneurons[27]. In control EP18 organotypic cultures, GAD65 immunostaining was low in putative GFP-labeled presynaptic boutons (**Fig. 4a,b**). In EndoN-treated basket cells, by contrast, GFP-labeled boutons showed a high degree of GAD65 colocalization (**Fig. 4c,d**), similar to what is observed for basket cells in mature organotypic cultures[27]. Quantitative analysis showed that 22% of boutons colocalized with GAD65 in untreated basket cells at EP18, and this percentage increased to 81% in cells treated with EndoN from EP14 to EP18 ($n = 110$ boutons from three control basket cells; $n = 138$ boutons from three EndoN-treated basket cells). GFP-labeled boutons of EP18 control basket cells most probably represent presynaptic terminals, even if they contain small amounts of GAD65.

To verify this notion, we co-transfected basket cells with P_{G67}-tdtomato and P_{G67}-synaptophysin-GFP (syn-GFP) to simultaneously visualize axon-bouton morphology and a synaptic marker. We found that 95.3% of tdtomato-labeled boutons contained syn-GFP in EP18 control cells (**Fig. 4e,f**; $n = 273$ boutons from three cells). The basket cell boutons with low GAD65 in control EP18 cortical slices probably released GABA that is mostly synthesized by GAD67. This glutamic acid decarboxylase is widely distributed in GABA neurons, including presynaptic terminals, and mediates most GABA synthesis[38]. Taken together, these results suggest that basket cell axons are competent to form perisomatic synapses between EP14 and EP18, but high concentrations of PSA inhibit the maturation of these synapses during this time period.

PSA removal promotes GABAergic synapse maturation *in vivo*

To substantiate these observations, we examined whether and how premature removal of PSA affects perisomatic innervation in the developing visual cortex *in vivo*. Maturation of perisomatic innervation in visual cortex has been previously quantified both by

immunohistochemistry of GAD65, as a synaptic marker, and through the use of transgenic mice in which basket axon terminals are specifically labeled[27,29]. Both approaches produced similar results and showed that perisomatic innervation significantly increases during the third and fourth postnatal week[27,29]. We focused our current study on perisomatic synapses surrounding layer 5 pyramidal cell somata; these synapses are largely derived from the parvalbumin-containing basket interneurons[30]. Mice were injected with either EndoN or vehicle (buffer) solution in visual cortex at P14 and analyzed at P18 (**Fig. 5a**,**b**). GABAergic synapses were identified by immunofluorescence labeling for both VGAT[39] (**Fig. 5c**) and GAD65 (**Supplementary Fig. 3** online), as GABAergic synaptic markers. In visual cortex injected with EndoN, the average number of VGAT- and GAD65-positive puncta around single neuronal soma increased by 36% and 46%, respectively, as compared with the contralateral uninjected cortex (**Fig. 5**; $n = 3$ mice; Mann-Whitney test, $P < 0.001$ for each mouse). Vehicle injection alone did not affect the density of perisomatic VGAT- and GAD65-positive puncta in the injected cortex as compared with the contralateral cortex ($n = 3$ mice; Mann-Whitney test, $P > 0.1$ in all cases). These results indicate that removal of PSA may promote maturation of perisomatic GABAergic innervation in adolescent visual cortex.

To examine whether premature removal of PSA increases GABAergic synaptic inhibition, we measured miniature inhibitory postsynaptic currents (mIPSCs) in visually identified layer 5 pyramidal neurons using whole-cell voltage clamp recordings (**Fig. 5d**). We compared the results from visual cortex injected with either vehicle or EndoN from P14 to P18. The decay kinetics of the mIPSCs was similar in the two groups (**Fig. 5e**; *t*-test, $P > 0.1$). The mean decay time constants were 21 ± 2 ms and 23 ± 2 ms, respectively, for EndoN-treated and control neurons. The frequency of mIPSCs was higher in EndoN-treated than in control neurons (**Fig. 5f**; 2.1 ± 0.2 Hz in control cells versus 2.9 ± 0.2 Hz in EndoN-treated cells; for both groups, $n = 18$ cells from four mice; *t*-test, $P < 0.01$), whereas the mean mIPSC amplitude did not differ significantly (**Fig. 5g**; *t*-test, $P > 0.1$). These results are consistent with a higher number of GABAergic synapses in the EndoN-treated cortex than in control visual cortex[28].

We investigated whether premature removal of PSA also affects excitatory transmission by measuring miniature excitatory postsynaptic currents (mEPSCs) in layer 5 pyramidal neurons (**Fig. 5h**). The decay kinetics of the mEPSCs was similar in the two groups (**Fig. 5i**; *t*-test, $P > 0.1$; mean decay time constant: 4.8 ± 0.3 ms and 5.1 ± 0.2 ms for control and EndoN-injected mice, respectively; $n = 20$ and 21 cells from four control and four EndoN-injected mice, respectively). EndoN treatment did not affect the frequency or the amplitude of mEPSCs (**Fig. 5j**,**k**; 0.9 ± 0.2 Hz in control cells versus 0.9 ± 0.2 Hz in EndoN-treated cells; *t*-test $P > 0.1$). Thus, the effects of premature PSA removal in this developmental window seem to be specific to GABAergic synapses.

PSA removal induces onset of critical period plasticity

Maturation of inhibition has been shown to regulate onset of the critical period for ocular dominance plasticity[24,25]. We investigated whether premature removal of PSA would induce a precocious onset of ocular dominance plasticity, as assessed by visual-evoked potential (VEP) recording (**Fig. 6** and **Supplementary Fig. 4** online). Eye-specific VEPs were recorded by alternatively closing the contralateral or the ipsilateral eye. The C/I VEP ratio indicates the relative strength of each eye input in driving the response of cortical neurons. In non-deprived control mice, both at P22 (**Fig. 6c**) and in adults[29], the VEP amplitude induced by stimulation of the contralateral eye is about three times larger than that of the ipsilateral eye, indicating a contralateral bias that is largely due to the predominance of crossed fibers in mouse retinal projections. Monocular deprivation of the contralateral eye for 5 d during a critical period (between P24 and P35 in mouse) results in weakening of its input in driving binocular cortical neurons, reflected as a decrease in the C/I VEP ratio[29]. Such ocular dominance plasticity cannot be induced by monocular deprivation before the critical period (for example, P17–P21; ref. 25).

We injected EndoN at P14 and examined the effects on the onset of ocular dominance plasticity by subsequent monocular deprivation from P17 to P22 (**Fig. 6a**). In EndoN-injected mice without monocular deprivation recorded at P22, the C/I VEP ratio was indistinguishable from that of vehicle-injected mice (mean ± s.e.m. C/I VEP = 2.9 ± 0.1 for EndoN-injected versus 3.0 ± 0.2 for vehicle-injected mice; $n = 3$ mice for both groups; Mann-Whitney test, $P < 0.1$); therefore, premature removal of PSA did not affect ocular dominance *per se*. In vehicle-injected mice, monocular deprivation from P17 to P21 did not result in a shift in ocular dominance (**Fig. 6c**; C/I VEP = 2.8 ± 0.2; $n = 6$ mice; *t*-test, $P < 0.1$). In EndoN-treated mice, by contrast, monocular deprivation between P17 and P21 induced a shift in the C/I VEP ratio from 3 to ~1.3 (**Fig. 6b**,**c**; C/I VEP = 1.3 ± 0.1; $n = 5$ mice; *t*-test, $P = 0.001$), which was probably due to a substantial reduction in VEP amplitude from the contralateral, deprived eye and an increase in VEP amplitudes of the ipsilateral, nondeprived eye[40]. The extent of this shift in ocular dominance is similar to that induced by monocular deprivation from P24 to P28 (the peak of the critical period) in control mice[29]. Therefore, premature removal of PSA in adolescent visual cortex induced precocious ocular dominance plasticity.

Previous studies have shown that enhancement of GABA transmission also results in a precocious onset of ocular dominance plasticity[25]. Expression of PSA might be either downstream of or in parallel to GABA transmission in its effect on ocular dominance plasticity. We therefore tested whether use-dependent enhancement of GABA transmission by diazepam treatment in visual cortex modulates PSA expression. Mice receiving a daily intraventricular injection of diazepam from P15 to P19, before the onset of the critical period, showed a marked decrease in cortical PSA, but not NCAM, as compared with vehicle-injected control mice (**Fig. 6d–f**; 34% average reduction in PSA expression; $n = 5$ diazepam-injected mice; $n = 3$ vehicle-injected mice; *t*-test, $P < 0.01$). These data suggest that GABA transmission might contribute to the endogenous activity-dependent mechanisms that modulate PSA and NCAM expression. Because removal of PSA in turn favors GABAergic synapse maturation, an increase in GABA transmission and removal of PSA may act synergistically to control the onset of ocular dominance plasticity.

DISCUSSION

Neocortical GABAergic circuits are characterized by heterogeneity in cell types[26], exquisite specificity in target innervation[34,41] and plasticity in synaptic connections[27,42]. Development of the mature GABAergic innervation pattern is achieved through the ordered progression of a series of morphogenic events that include cell migration, axon growth and branching, synapse formation and refinement. Cell adhesion regulated by both genetic programs and neural activity is probably central to the establishment and plasticity of GABAergic innervation patterns. As a widespread and general modulator of cell interaction, PSA in itself is unlikely to provide a specific signal for axon-target interactions[2]. Instead, its expression may represent a regulated permissive signal for producing optimal interactions between selected GABAergic axons and their cellular targets or extracellular matrix, which may either promote or inhibit specific morphogenic events at the appropriate time and in the correct order.

Basket interneurons in visual cortex show characteristic axon arbor size and geometry and exuberant local innervation of the perisomatic region of pyramidal neurons[34,41]. This pattern of innervation is established during an extended postnatal period involving sequential and overlapping progression of axon growth, branching and synapse formation[27]. The increase in exuberant local axon branching and perisomatic innervation is most pronounced in the fourth postnatal week, concurrent with the maturation of functional GABAergic inhibition[27,28]. Here we found that EndoN-treated basket cell axons were in fact already highly competent in perisomatic synapse formation at least a week earlier, when basket cells normally are still actively elaborating their axon arbors. Indeed, early perisomatic synapse formation can be triggered by premature removal of PSA in the third week. It is possible that excessive premature synapse formation might constrain axon growth. Higher expression of PSA during the first two postnatal weeks thus may hinder interactions between basket cell axon and pyramidal neurons and hold off perisomatic synapse formation, thereby preferentially promoting the proper elaboration of basket cell axon arbors. Subsequent activity-dependent removal of PSA may unmask mechanisms that are already in place along basket cell axons for synapse formation. Such a 'ready-to-synapse' state of basket cell axons may allow fast responses to local synaptogenic cues immediately after PSA removal. Our study thus identifies a function of PSA in the activity-dependent maturation of perisomatic innervation during cortical circuit development in the adolescent brain. It is likely that maturation of the GABAergic synapse is regulated by those PSA molecules localized around GABAergic axon terminals (**Supplementary Fig. 2**) and is less dependent on the overall amounts of PSA in the cortex. Our analysis of mIPSCs in EndoN-treated visual cortex did not distinguish among different classes of GABAergic input; as a result, we cannot exclude the possibility that removal of PSA may also promote the formation of other classes of GABAergic synapses, in addition to perisomatic synapses.

We also found that PSA has a role in regulating the onset of ocular dominance plasticity. Because maturation of GABAergic inhibition promotes the onset of ocular dominance plasticity[24,25], the effects of PSA removal on GABAergic inhibition probably contribute to its impact on ocular dominance plasticity. Removal of PSA, however, might also regulate the formation and function of glutamatergic synapses[14,16] and neuron-glia interactions[17]. Our mEPSC recordings suggest that a precocious decline of PSA does not affect this aspect of excitatory transmission in this specific developmental window, but we cannot exclude the possibility that PSA expression may also influence ocular dominance plasticity through mechanisms parallel to promoting the maturation of GABAergic inhibition.

The cellular mechanism that couples neural activity and PSA expression is central to linking this general modulator of cell interaction to specific neural developmental events. Although PSA is widely expressed throughout the visual cortex, it is unknown whether it is also preferentially localized to particular cellular and subcellular surfaces, such as basket cell axons, pyramidal cell somata and astrocytes. The downregulation of PSA might be achieved by a decrease in the expression[43,44] and activity of the two polysialyltransferases, ST8SiaII (also known as STX) and ST8SiaIV (PST), responsible for its synthesis[45]. In addition, PSA expression on the cell surface can be more locally and rapidly regulated by activity-dependent trafficking of PSA-NCAM[46,47]. We have shown here that enhanced GABA signaling through diazepam-sensitive receptors downregulates PSA expression in visual cortex (**Fig. 6**), although the cellular mechanism involved is unclear. GABA signaling is implicated both in the maturation of GABAergic innervation[30] and in the onset of the critical period for ocular dominance plasticity[24,25]. Because removal of PSA further promotes GABAergic synapse formation and GABA transmission (**Figs. 3–5**), GABA signaling and PSA removal may constitute a positive feedback mechanism to accelerate synapse formation once a threshold of GABA transmission is reached. In addition to homophilic NCAM binding, removal of PSA regulates various adhesion and signaling receptors such as cadherins, L1CAMs, integrins[4], FGF receptors[14] and trkB[48]. Such activity-dependent exposure and modulation of adhesion and signaling molecules may sharpen the specificity and sequential order of cell-cell interactions to sculpt neuronal connections in complex tissues such as neocortical circuits.

Although PSA is widely expressed in the developing CNS, studies of ST8SiaII and ST8SiaIV single-knockout mice have revealed no gross alterations of cortical morphology[15,49]. Deficits in synaptic transmission and plasticity have been reproducibly reported in these mutant mice, however, suggesting that there are 'subtle' alterations in synapse formation and neural circuits. In addition, mice lacking both ST8SiaII and ST8SiaIV show marked defects in the brain and early lethality[50]. These defects are selectively rescued by the additional deletion of NCAM, suggesting that the marked phenotype in the double knockout mice originates from a gain of NCAM functions at the wrong developmental stages caused by PSA deficiency. These data are consistent with the idea that PSA is involved in controlling the timing of specific molecular and cellular interactions that mediate neuronal morphogenesis. Our study on specific types of GABAergic synapse now demonstrates that PSA has an important role in their structural and functional maturation. Similar high-resolution analysis of specific neuronal connections at defined developmental stages will probably reveal additional functions of PSA in fine-tuning the spatial and temporal control of neural circuit development.

METHODS

Analysis of PSA and NCAM in visual cortex. Mice were anesthetized with sodium pentobarbitone (6 mg per 100 g of body weight) and transcardially perfused with 4% paraformaldehyde in phosphate buffer (pH 7.4). Coronal sections (80-μm thick) were cut from visual cortex with a vibratome (Leica VT100). Brain sections were blocked in 10% normal goat serum (NGS) and 1% Triton X-100. Slices were then incubated overnight at 4 °C in 10% NGS, 0.1% Triton X-100 and either a monoclonal antibody to PSA (dilution 1:500; cat. no. MAB5324, Chemicon) or a rabbit antibody to NCAM (1:500; cat. no. AB5032, Chemicon). Sections were then incubated with the appropriate Alexa594-conjugated goat IgG (1:400; Molecular Probes) and mounted.

Visual cortices from at least three mice were analyzed for each developmental age and experimental condition, and three coronal sections containing the primary visual cortex were analyzed from each mouse. Binocular region of primary visual cortex was identified by anatomical landmarks. We acquired images from a single confocal plane in layer 5/6 and layer 2/3 with a ×20 objective using a confocal microscope (Zeiss LSM510). Images were acquired with the same acquisition parameters for all samples, saved as TIFF files, and analyzed with ImageJ software. For monocular TTX-injected mice, both the ipsilateral (nondeprived) and contralateral (deprived) cortex were analyzed and compared in each mouse. Fluorescence intensity values were quantified separately in layers 5/6 and 2/3. Whereas the signal intensity for PSA was lower in layer 2/3 than in layer 5/6, the ratio between expression in DR versus LR mice was similar for both the infra- and supragranular layers. The same was true for the ratio of PSA in the cortex contralateral to the TTX-injected eye and the ipsilateral cortex. In the text we show quantification data only for layer 5/6 (**Figs. 2b** and **6e**).

All quantifications were done blind to the age of the mice, rearing condition or treatment, and were repeated by two different operators.

Immunoblotting. Protein lysates were prepared by homogenizing tissue from either mouse visual cortex or cortical organotypic cultures in 50 mM Tris-HCl (pH 7.6), 150 mM NaCl, 2 mM EDTA, 1% Igepal C-630 and 1× protease

inhibitor cocktail (Roche). For *in vivo* analysis, at least two mice for each age point were used; for cultures, 4–6 slices were collected and pooled together for each developmental time point. Tissues were disrupted with needles and a syringe. Protein was quantified by Bradford protein assay (cat. no. 500-0006, Bio-Rad), and samples were adjusted to equivalent levels with deionized water. Samples were mixed with an equal volume of 2× Laemmli buffer, boiled for 5 min, and either used immediately or stored at −80 °C. Equal amounts were loaded in each lane. Proteins were separated by using 6.5% polyacrylamide separation gels with 5% stacking gels (Bio-Rad), and were transferred onto Millipore Immobilon-P PVDF membrane, which was then blocked by incubation in TBS with 5% dried milk and 0.1% Tween-20. We probed membranes with anti-PSA (1:1,000, mouse monoclonal IgM; cat. no. MAB5324, Chemicon) and anti–β-actin (1:5,000, mouse monoclonal IgG; cat. no. NB.600.501, Novus Biological). Horseradish peroxidase–conjugated anti-mouse secondary antibody (Invitrogen, Amersham) was then added to the blots. Immunoreactive bands were detected with Western Lightning Plus Chemiluminescence Reagent (cat. no. NEL103, Perkin-Elmer), and signals were visualized by exposing the membrane to Bioflex MSI autoradiography or X-ray film (Intersciences). To normalize the amount of PSA to β-actin, we scanned nonsaturating exposures of immunoblots and analyzed band intensities with ImageJ software.

Analysis of perisomatic innervation in organotypic slices. Preparation of slice cultures has been described[27]. In experiments in which PSA was prematurely reduced, EndoN (2 U/ml) was added to the culture medium during the indicated time window. For biolistic transfection, cells were transfected with the Gene Gun system (Bio-Rad). The age of the culture is reported as equivalent postnatal day (EP); for example, EP13 for cultures prepared from P4 mice means P4 + 9 d *in vitro*.

For immunohistochemistry, imaging and analysis, slices were fixed, freeze-thawed and immunostained as described[27,30]. We used mouse monoclonal antibodies to NeuN (1:400; cat. no. MAB377, Chemicon) and GAD65 (1:1,000; cat. no. MAB351R, Chemicon). Confocal imaging and data analysis were performed as described[27,30]. See **Supplementary Methods** online for details.

Mouse treatment. Intravitreal TTX injections (3 mM TTX in 0.02 M citrate buffer; Alomone Labs) were performed daily under fluothane anesthesia with a micropipette connected to a microinjector. The micropipette was inserted at the ora serrata and the injection volume (less than 1 μl) was slowly released. Blockade of retinal activity was monitored by observing tonic dilation of the pupil and loss of direct and indirect pupillary response to eye illumination.

For intracortical injections, P14 C57BL/6 mouse pups were anesthetized with ketamine (0.56 mg per g) and xylazine (0.03 mg per g), and mounted on a stereotaxic frame. After incision of the skin overlying the skull, a small hole was made directly over the left hemisphere in the visual cortex. A micropipette attached to a Picospritzer was inserted to a depth of 0.5 mm below the pia. We injected 1.0 μl of EndoN (2 U/μl in saline) or vehicle (saline) in at least four different sites with 15 p.s.i. at a frequency of 0.3 Hz.

For intraventricular injections, mouse pups were injected with diazepam (2 mg/ml in 50% propylene glycol) or vehicle (50% propylene glycol) once a day from P15 to P18. Mice were anesthetized with ketamine (0.56 mg per g) and xylazine (0.03 mg per g) and mounted on a stereotaxic frame. After incision of the skin overlying the skull, a small hole was made directly behind the bregma, <1 mm from the medial line. A micropipette attached to a Picospritzer was inserted to a depth of 1.5 mm below the pia. We injected 1.5 μl of diazepam or vehicle. The position of the ventricle was initially verified by 1,1′-dioctadecyl-3,3,3′,3′-tetramethylindocarbocyanine percholate (DiI) injection.

Analysis of perisomatic innervation in visual cortex. At P14, mice were injected with either EndoN (~1 μl; 2 U/μl in saline) or vehicle (saline) in the primary visual cortex. At P18, mice were anesthetized and perfused transcardially with 4% paraformaldehyde in phosphate buffer (pH 7.4). Immunohistochemistry, confocal imaging and analysis of perisomatic innervation were performed as described[27,30]. For details, see **Supplementary Methods**.

mPSC recording. At P14, mice were injected with either EndoN (~1 μl; 2 U/μl in saline) or vehicle solution (saline) in the primary visual cortex. Mice were then killed between P17 and P19, and mPSCs were recorded from layer 5 pyramidal cells in V1. In brief, brain slices (300-μm thick) were cut in the coronal plane with a Vibroslicer (Vibratome) in ice-cold dissection artificial cerebrospinal fluid (ACSF) containing (in mM) 212.7 sucrose, 2.5 KCl, 1.25 NaH_2PO_4, 3 $MgSO_4$, 1 $CaCl_2$, 10 D-(+)-glucose and 26 $NaCHO_3$ continuously bubbled with 95% O_2/5% CO_2, and then allowed to recover for >30 min in normal ACSF containing (in mM) 126 NaCl, 2.5 KCl, 1.25 NaH_2PO_4, 1 $MgSO_4$, 2 $CaCl_2$, 10 D-(+)-glucose and 25 $NaCHO_3$ continuously bubbled with 95% O_2/5% CO_2. The slices were then transferred to the recording chamber, submerged in normal ACSF, and perfused at a rate of 2–3 ml/min (25 ± 1 °C). Slices were viewed with infrared differential interference contrast optics on an upright microscope (Axioskop, Zeiss). Whole-cell voltage clamp in visually identified layer 5 pyramidal neurons was performed with a Multiclamp 700A amplifier (Axon Instruments). Signals were filtered with a 2-kHz low pass filter and sampled at 5 kHz by a pClamp9 program and DigiData interface. Patch pipettes (2–4 MΩ) were filled with (in mM) 115 $CsMeSO_3$, 20 CsCl, 10 HEPES, 2.5 $MgCl_2$, 4 Na_2ATP, 0.4 NaGTP, 10 sodium phosphocreatine and 0.6 EGTA. All recordings were done at 25 °C.

Only cells with a series resistance of <30 MΩ and showing steady mPSC amplitude during all of the recording period were studied. mIPSCs were recorded in presence of (in μm) 1 TTX, 50 APV and 20 CNQX. mEPSCs were recorded in presence of (in μm) 1 TTX, 50 APV and 100 picrotoxin. The recordings were done at 0 mV for mIPSCs and −60 mV for mEPSCs. For each cell, mPSCs were collected over a period of 6 min. Analysis was performed with a template matching AxoGraph software (Axon Instruments). Only events with a rise time of 0.5–8 ms for mIPSCs and 0.2–5 ms for mEPSCs were considered. For the determination of frequency, we considered all recorded events that were at least 10 ms apart in a single cell. For the determination of amplitude, we considered for each cell events that were not superimposed. We estimated that, to satisfy this criterion, mIPSC and mEPSC events have to be at least 120-ms and 30-ms apart, respectively. For each cell, the rise time and decay constant were calculated from the average of the first 150 isolated events for mIPSCs and that of the first 100 isolated events for mEPSCs. For calculating the decay time constant, the data were fitted with a single exponential.

VEP recording. We carried out VEP recording in mice as described[29]. All measurements were performed in the primary binocular visual cortex 10–20° from the vertical meridian in anesthetized mice. In brief, a large portion of the skull (4 × 4 mm^2) overlying the visual cortex was carefully drilled and removed to leave the dura intact. A resin-coated microelectrode (WPI, Sarasota) with a tip impedance of 0.5 MΩ was inserted into the cortex perpendicular to the stereotaxic plane. Microelectrodes were inserted 2.7–2.9 mm lateral to lambda. Recordings were performed at a depth of 400 μm from the pia, where VEPs had their maximal amplitude. Electrical signals were amplified (50,000-fold), band-pass filtered (0.3–100 Hz, −6 dB/oct), digitized (12-bit resolution), and averaged (at least 128 events in blocks of 16 events each) in synchrony with the stimulus contrast reversal. The visual stimulus was a horizontal optimal sinusoidal grating (0.05 c/°, contrast 90%, mean luminance 15 cd/m^2), reversed in contrast sinusoidally at 0.5 Hz generated by a VSG2/2 card (Cambridge Research System) by custom software and presented on the face of a TV display (Barco CCID 7751) suitably linearized by gamma correction. Transient VEPs in response to abrupt contrast reversal were evaluated in the time domain by measuring the peak-to-trough amplitude and peak latency of the principal negative component.

To assess the onset of the critical period for monocular deprivation, P17 mice were anesthetized intraperitoneally with avertin (tribromoethanol in amylene hydrate, 0.2 μl per g). Lid margins were trimmed and sutured with 7-0 silk. Mice were allowed to recover from anesthesia and were returned to their cages. The effectiveness of lid closure was checked daily. Mice that showed occasional lid reopening were not included in the experiments. We assessed the effects of monocular deprivation by VEP recordings 4–5 d after eyelid suture. Immediately before the recording session, the lids were cut and the eye was washed with saline and carefully inspected to verify that the surgical procedure had not caused any damage. The relative contribution of the two eyes to cortical responses was defined as the amplitude ratio between the responses to stimulation of the contralateral eye and those of the ipsilateral eye (C/I VEP). For each mouse, the contralateral to ipsilateral amplitude ratio was evaluated by integrating responses recorded at three different locations in the binocular visual cortex.

Statistical analysis. Differences between groups were assessed with the Kruskal-Wallis one-way ANOVA on ranks with Dunn's *post hoc* test for data that are not normally distributed. Differences between two experimental groups were assessed with the Mann-Whitney test for data that are not normally distributed and with the *t*-test for data that are normally distributed.

Note: Supplementary information is available on the Nature Neuroscience website.

ACKNOWLEDGMENTS

We thank P. Wu, E. Putignano, N. Berardi and J. Boehm for technical assistance and discussion; and E. Ruthazer for critically reading the manuscript. This work was supported by the National Institutes of Health (RO1 EY 13564-01). G.D.C. has a National Association for Research in Schizophrenia and Depression (NARSAD) Young Investigator Award founded by the Forrest C. Lattner Foundation. Z.J.H. is a Pew and McKnight Scholar.

AUTHOR CONTRIBUTIONS

G.D.C. and Z.J.H. conceived and organized the project and wrote the manuscript. G.D.C. conducted most of the experiments. B.C. contributed to the *in vitro* and *in vivo* morphological studies. S.J.K. and Y.F. carried out the mPSC recordings. M.-C.B. performed the western blotting. C.Z.W. contributed to the PSA expression analysis *in vivo*. U.R. provided endoN and advice. L.M. provided the facility for dark rearing and VEP recording.

Published online at http://www.nature.com/natureneuroscience
Reprints and permissions information is available online at http://npg.nature.com/reprintsandpermissions

1. Rothbard, J.B., Brackenbury, R., Cunningham, B.A. & Edelman, G.M. Differences in the carbohydrate structures of neural cell-adhesion molecules from adult and embryonic chicken brains. *J. Biol. Chem.* **257**, 11064–11069 (1982).
2. Johnson, C.P., Fujimoto, I., Rutishauser, U. & Leckband, D.E. Direct evidence that neural cell adhesion molecule (NCAM) polysialylation increases intermembrane repulsion and abrogates adhesion. *J. Biol. Chem.* **280**, 137–145 (2005).
3. Acheson, A., Sunshine, J.L. & Rutishauser, U. NCAM polysialic acid can regulate both cell-cell and cell-substrate interactions. *J. Cell Biol.* **114**, 143–153 (1991).
4. Fujimoto, I., Bruses, J.L. & Rutishauser, U. Regulation of cell adhesion by polysialic acid. Effects on cadherin, immunoglobulin cell adhesion molecule and integrin function and independence from neural cell adhesion molecule binding or signaling activity. *J. Biol. Chem.* **276**, 31745–31751 (2001).
5. Ono, K., Tomasiewicz, H., Magnuson, T. & Rutishauser, U. N-CAM mutation inhibits tangential neuronal migration and is phenocopied by enzymatic removal of polysialic acid. *Neuron* **13**, 595–609 (1994).
6. Nait-Oumesmar, B. *et al.* Progenitor cells of the adult mouse subventricular zone proliferate, migrate and differentiate into oligodendrocytes after demyelination. *Eur. J. Neurosci.* **11**, 4357–4366 (1999).
7. O'Leary, D.D. & Terashima, T. Cortical axons branch to multiple subcortical targets by interstitial axon budding: implications for target recognition and 'waiting periods'. *Neuron* **1**, 901–910 (1988).
8. Seki, T. & Rutishauser, U. Removal of polysialic acid-neural cell adhesion molecule induces aberrant mossy fiber innervation and ectopic synaptogenesis in the hippocampus. *J. Neurosci.* **18**, 3757–3766 (1998).
9. Tang, J., Landmesser, L. & Rutishauser, U. Polysialic acid influences specific pathfinding by avian motoneurons. *Neuron* **8**, 1031–1044 (1992).
10. Tang, J., Rutishauser, U. & Landmesser, L. Polysialic acid regulates growth cone behavior during sorting of motor axons in the plexus region. *Neuron* **13**, 405–414 (1994).
11. Yamamoto, N. *et al.* Inhibitory mechanism by polysialic acid for lamina-specific branch formation of thalamocortical axons. *J. Neurosci.* **20**, 9145–9151 (2000).
12. Yin, X., Watanabe, M. & Rutishauser, U. Effect of polysialic acid on the behavior of retinal ganglion cell axons during growth into the optic tract and tectum. *Development* **121**, 3439–3446 (1995).
13. El Maarouf, A. & Rutishauser, U. Removal of polysialic acid induces aberrant pathways, synaptic vesicle distribution and terminal arborization of retinotectal axons. *J. Comp. Neurol.* **460**, 203–211 (2003).
14. Dityatev, A. *et al.* Polysialylated neural cell adhesion molecule promotes remodeling and formation of hippocampal synapses. *J. Neurosci.* **24**, 9372–9382 (2004).
15. Eckhardt, M. *et al.* Mice deficient in the polysialyltransferase ST8SiaIV/PST-1 allow discrimination of the roles of neural cell adhesion molecule protein and polysialic acid in neural development and synaptic plasticity. *J. Neurosci.* **20**, 5234–5244 (2000).
16. Muller, D. *et al.* PSA-NCAM is required for activity-induced synaptic plasticity. *Neuron* **17**, 413–422 (1996).
17. Theodosis, D.T., Bonhomme, R., Vitiello, S., Rougon, G. & Poulain, D.A. Cell surface expression of polysialic acid on NCAM is a prerequisite for activity-dependent morphological neuronal and glial plasticity. *J. Neurosci.* **19**, 10228–10236 (1999).
18. Bruses, J.L. & Rutishauser, U. Roles, regulation and mechanism of polysialic acid function during neural development. *Biochimie* **83**, 635–643 (2001).
19. Swadlow, H.A. Fast-spike interneurons and feedforward inhibition in awake sensory neocortex. *Cereb. Cortex* **13**, 25–32 (2003).
20. Pouille, F. & Scanziani, M. Enforcement of temporal fidelity in pyramidal cells by somatic feed-forward inhibition. *Science* **293**, 1159–1163 (2001).
21. Hasenstaub, A. *et al.* Inhibitory postsynaptic potentials carry synchronized frequency information in active cortical networks. *Neuron* **47**, 423–435 (2005).
22. Somogyi, P. & Klausberger, T. Defined types of cortical interneurone structure space and spike timing in the hippocampus. *J. Physiol. (Lond.)* **562**, 9–26 (2005).
23. Hensch, T.K. Critical period plasticity in local cortical circuits. *Nat. Rev. Neurosci.* **6**, 877–888 (2005).
24. Hanover, J.L., Huang, Z.J., Tonegawa, S. & Stryker, M.P. Brain-derived neurotrophic factor overexpression induces precocious critical period in mouse visual cortex. *J. Neurosci.* **19**, RC40 (1999).
25. Fagiolini, M. & Hensch, T.K. Inhibitory threshold for critical-period activation in primary visual cortex. *Nature* **404**, 183–186 (2000).
26. Markram, H. *et al.* Interneurons of the neocortical inhibitory system. *Nat. Rev. Neurosci.* **5**, 793–807 (2004).
27. Chattopadhyaya, B. *et al.* Experience and activity-dependent maturation of perisomatic GABAergic innervation in primary visual cortex during a postnatal critical period. *J. Neurosci.* **24**, 9598–9611 (2004).
28. Morales, B., Choi, S.Y. & Kirkwood, A. Dark rearing alters the development of GABAergic transmission in visual cortex. *J. Neurosci.* **22**, 8084–8090 (2002).
29. Huang, Z.J. *et al.* BDNF regulates the maturation of inhibition and the critical period of plasticity in mouse visual cortex. *Cell* **98**, 739–755 (1999).
30. Chattopadhyaya, B. *et al.* GAD67-mediated GABA synthesis and signaling regulate inhibitory synaptic innervation in the visual cortex. *Neuron* **54**, 889–903 (2007).
31. Toki, S. *et al.* Importance of early lighting conditions in maternal care by dam as well as anxiety and memory later in life of offspring. *Eur. J. Neurosci.* **25**, 815–829 (2007).
32. Rutishauser, U., Watanabe, M., Silver, J., Troy, F.A. & Vimr, E.R. Specific alteration of NCAM-mediated cell adhesion by an endoneuraminidase. *J. Cell Biol.* **101**, 1842–1849 (1985).
33. Klostermann, O. & Wahle, P. Patterns of spontaneous activity and morphology of interneuron types in organotypic cortex and thalamus-cortex cultures. *Neuroscience* **92**, 1243–1259 (1999).
34. Di Cristo, G. *et al.* Subcellular domain–restricted GABAergic innervation in primary visual cortex in the absence of sensory and thalamic inputs. *Nat. Neurosci.* **7**, 1184–1186 (2004).
35. Echevarria, D. & Albus, K. Activity-dependent development of spontaneous bioelectric activity in organotypic cultures of rat occipital cortex. *Brain Res. Dev. Brain Res.* **123**, 151–164 (2000).
36. Dupuy, S.T. & Houser, C.R. Prominent expression of two forms of glutamate decarboxylase in the embryonic and early postnatal rat hippocampal formation. *J. Neurosci.* **16**, 6919–6932 (1996).
37. Tian, N. *et al.* The role of the synthetic enzyme GAD65 in the control of neuronal γ-aminobutyric acid release. *Proc. Natl. Acad. Sci. USA* **96**, 12911–12916 (1999).
38. Asada, H. *et al.* Cleft palate and decreased brain gamma-aminobutyric acid in mice lacking the 67-kDa isoform of glutamic acid decarboxylase. *Proc. Natl. Acad. Sci. USA* **94**, 6496–6499 (1997).
39. Minelli, A., Alonso-Nanclares, L., Edwards, R.H., DeFelipe, J. & Conti, F. Postnatal development of the vesicular GABA transporter in rat cerebral cortex. *Neuroscience* **117**, 337–346 (2003).
40. Frenkel, M.Y. & Bear, M.F. How monocular deprivation shifts ocular dominance in visual cortex of young mice. *Neuron* **44**, 917–923 (2004).
41. Somogyi, P., Tamas, G., Lujan, R. & Buhl, E.H. Salient features of synaptic organization in the cerebral cortex. *Brain Res. Brain Res. Rev.* **26**, 113–135 (1998).
42. Knott, G.W., Quairiaux, C., Genoud, C. & Welker, E. Formation of dendritic spines with GABAergic synapses induced by whisker stimulation in adult mice. *Neuron* **34**, 265–273 (2002).
43. Kurosawa, N., Yoshida, Y., Kojima, N. & Tsuji, S. Polysialic acid synthase (ST8Sia II/STX) mRNA expression in the developing mouse central nervous system. *J. Neurochem.* **69**, 494–503 (1997).
44. Soares, S., von Boxberg, Y., Ravaille-Veron, M., Vincent, J.D. & Nothias, F. Morphofunctional plasticity in the adult hypothalamus induces regulation of polysialic acid–neural cell adhesion molecule through changing activity and expression levels of polysialyltransferases. *J. Neurosci.* **20**, 2551–2557 (2000).
45. Angata, K. & Fukuda, M. Polysialyltransferases: major players in polysialic acid synthesis on the neural cell adhesion molecule. *Biochimie* **85**, 195–206 (2003).
46. Bouzioukh, F., Tell, F., Jean, A. & Rougon, G. NMDA receptor and nitric oxide synthase activation regulate polysialylated neural cell adhesion molecule expression in adult brainstem synapses. *J. Neurosci.* **21**, 4721–4730 (2001).
47. Bruses, J.L. & Rutishauser, U. Regulation of neural cell adhesion molecule polysialylation: evidence for nontranscriptional control and sensitivity to an intracellular pool of calcium. *J. Cell Biol.* **140**, 1177–1186 (1998).
48. Muller, D. *et al.* Brain-derived neurotrophic factor restores long-term potentiation in polysialic acid–neural cell adhesion molecule-deficient hippocampus. *Proc. Natl. Acad. Sci. USA* **97**, 4315–4320 (2000).
49. Angata, K. *et al.* Sialyltransferase ST8Sia-II assembles a subset of polysialic acid that directs hippocampal axonal targeting and promotes fear behavior. *J. Biol. Chem.* **279**, 32603–32613 (2004).
50. Weinhold, B. *et al.* Genetic ablation of polysialic acid causes severe neurodevelopmental defects rescued by deletion of the neural cell adhesion molecule. *J. Biol. Chem.* **280**, 42971–42977 (2005).